Covalent-organic framework nanobionics for robust cytoprotection

Jieying Liang,*[†a] Qianfan Chen,[†b] Joel Yong[a], Hiroki Suyama,[c] Joanna Biazik,[d] Bosiljka Njegic,[e] Aditya Rawal,[e] Kang Liang*[a,b]

[a]School of Chemical Engineering and Australian Centre for NanoMedicine, The University of New South Wales, Sydney, NSW 2052, Australia

[b]Graduate School of Biomedical Engineering, The University of New South Wales, Sydney, NSW 2052, Australia

[c]UNSW RNA Institute, The University of New South Wales, Sydney, NSW 2052, Australia

[d]Electron Microscope Unit, Mark Wainwright Analytical Centre, The University of New South Wales, NSW 2052, Australia

[e]Nuclear Magnetic Resonance Facility, Mark Wainwright Analytical Centre, University of New South Wales, Sydney, NSW, 2052 Australia

[†]The authors contributed equally in this work

*Email: jieying.liang@unsw.edu.au; kang.liang@unsw.edu.au

Samples	**BET surface area (**m^2/g**)**	**Total pore volume (**cm^3/g**)**	**pore size** (nm)
COF[1]	73.5	0.42	1.89
Yeast	3.2	0.03	8.3
Yeast-COF	22.5	0.13	12.6

Table S1. The N_2 physisorption isotherms yeast and yeast-COF, and their pore sizes.

Table S2. The downregulated and upregulated genes of yeast-COF compared to native yeast and their functional analysis.

Downregulated genes	Functional analysis
YPR170C	
YER067C-A	
YKL136W	Unknown or predicted nonfunctionally
YGR039W	
YGL118C	
YOL058W	
snR39B	Ribosome and amino acid biosynthesis
TL(CAA)L	
YHR136C	kinase inhibitor
Upregulated genes	
YIL053W	
YDR044W	A possible disruption to the oxygen availability
YBR085W	
YBR054W	
YGL008C	Stress responses
YLL024C	
YJL045W	Links the tricarboxylic acid (TCA) cycle and the electron transport chain
YNL117W	Involved in the glyoxylate bypass of the full TCA cycle
Others	Related to amino acid biosynthesis

Nanoshell composition	Properties	Ref.
COF	Induced a superior protection against high temperature (100 °C) and acid condition (pH 2). Furth catalase coating enables yeast fermentation and ethanol production even under strong oxidative stress.	This work
ZIF-8	Induced the yeast cell hibernation state.	[2]
ZIF-8	Nanocoating with β-galactosidase allowed yeast to survive in nutrient-depleted environments.	[3]
MOF $[Zr_6O_4(OH)_4(BTB)_2(OH)_6(H_2O)_6]$	Enhanced the lifetime of anaerobes in the presence of O_2, and maintains the continuous production of acetic acid from CO_2.	[4]
ZIF-8	Allow mass and energy exchange between chloroplasts and the environment, and protect chloroplasts from microbiological degradation.	[5]
Metal–Polyphenol Nanoshell	Enabled controllably degraded on-demand, while protected the yeast from multiple external aggressors, including UV irradiation, lytic enzymes, and silver nanoparticles.	[6]
Alginate/Polydopamine Core/Shell Microcapsules	Prevented gel swelling and cell leakage, and increased resistance against enzymatic attack and UV irradiation.	[7]
SiO_2	Enhanced defense against high temperature (49 to 53 °C).	[8]
SiO_2–TiO_2	Controlled the cell division and effectively dissipated heat energy.	[9]
Polyelectrolytes/Multiwalled Carbon Nanotubes	Affected the electron mediation between the encapsulated yeast cells and the artificial electron acceptor.	[10]

Table S3. Comparison of yeast-COF system to the other reported system.

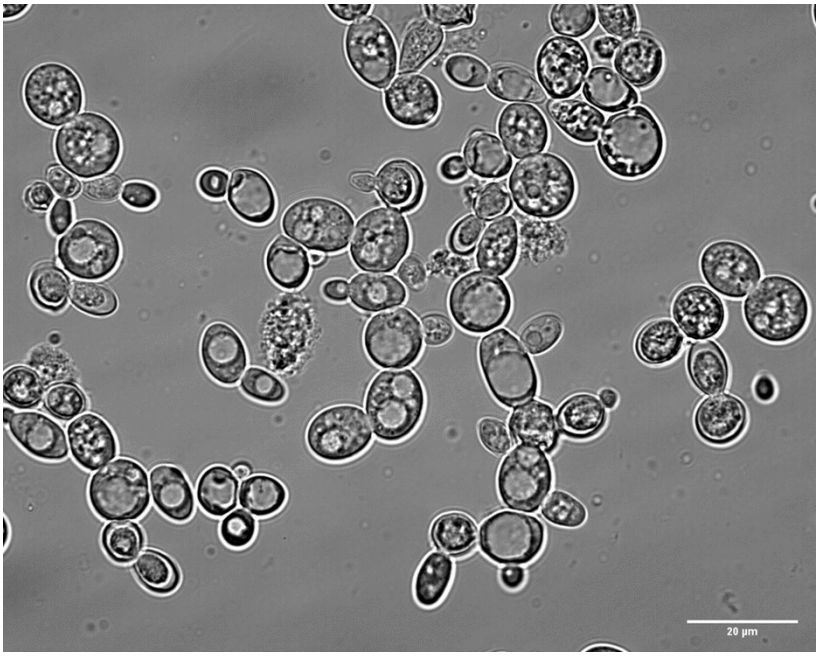

Figure S1. Optical micrograph of native yeast.

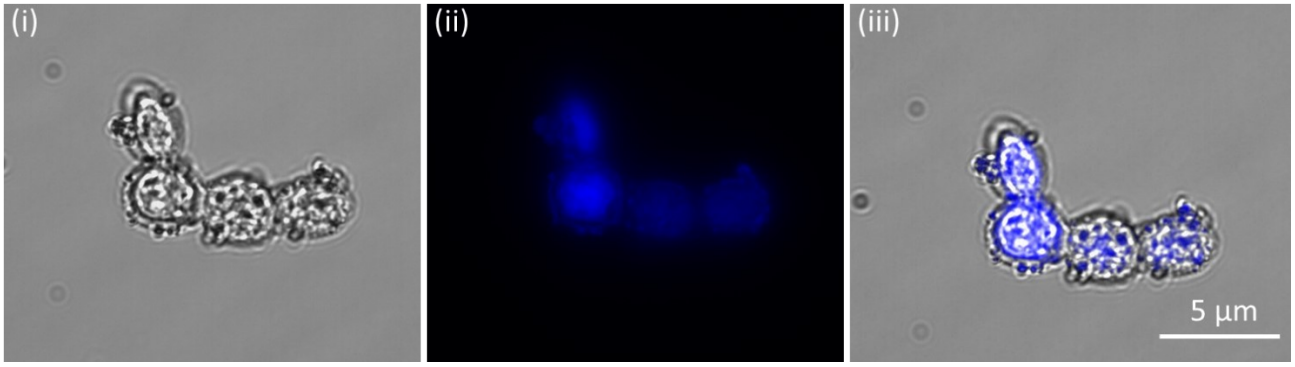

Figure S2. The homogeneous formation of the COF-LZU1-based exoskeleton around yeast. (i) Bright field image; (ii) Fluorescent image of Alexa Fluor 350-labelled COF-LZU1 (blue); (iii) The overlay of image of (i) and (ii).

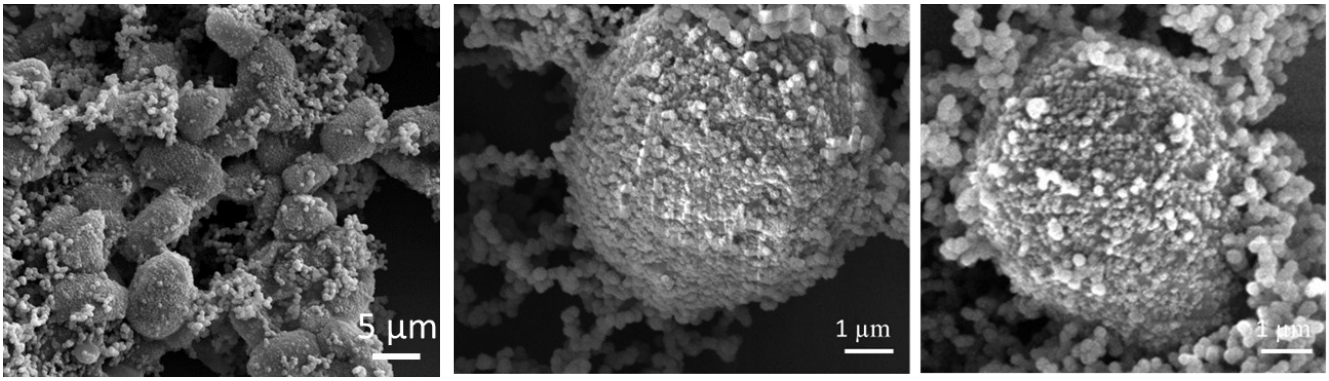

Figure S3. SEM images of yeast-COF.

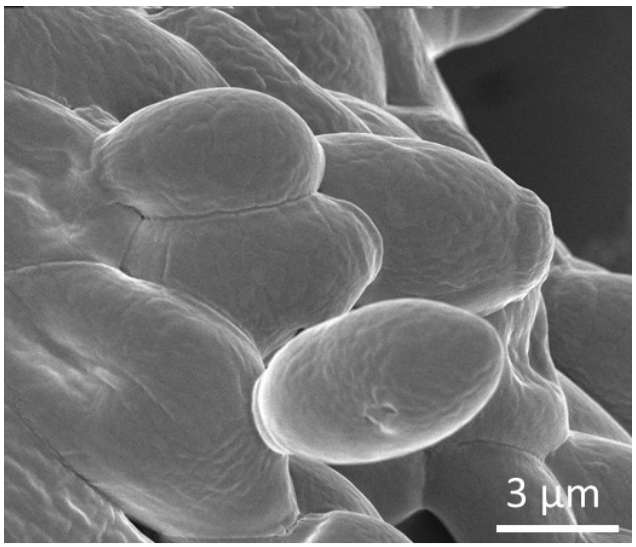

Figure S4. SEM image of native yeast cells.

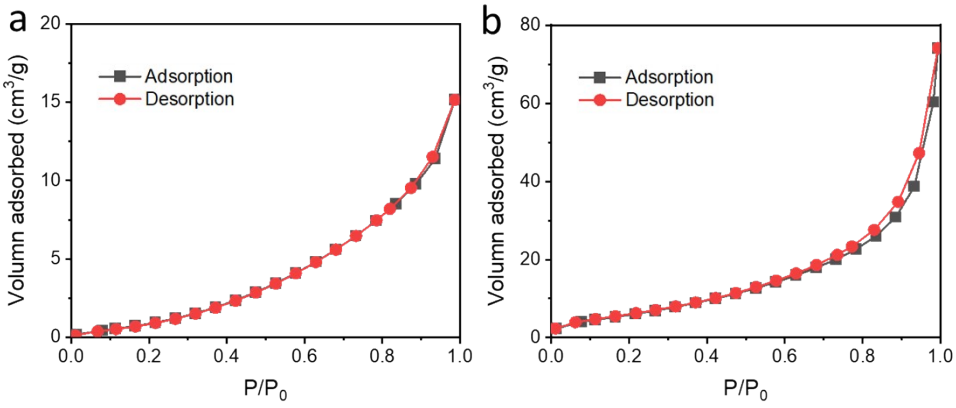

Figure S5. N_2 adsorption isotherm at 77 K of (a) yeast, (b) yeast-COF.

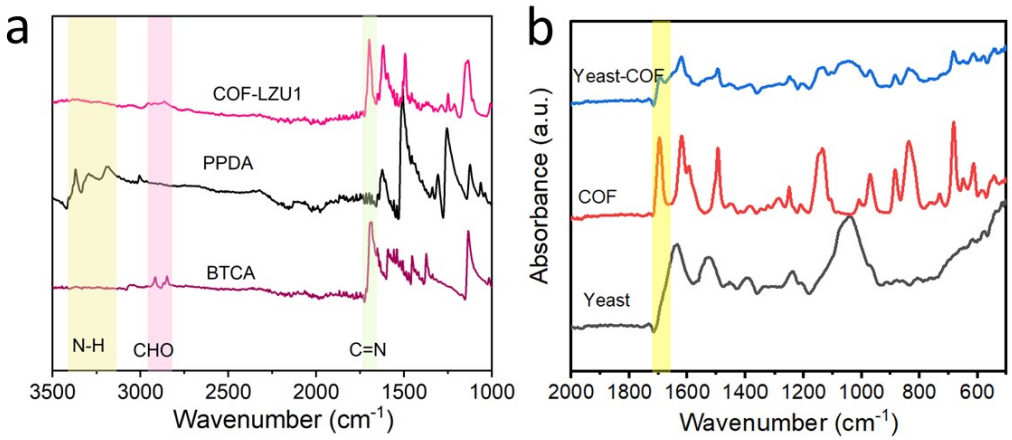

Figure S6. (a) FTIR spectra of BTCA, PDDA and COF-LZU1; (b) FTIR spectra of native yeast, COF, and yeast-COF.

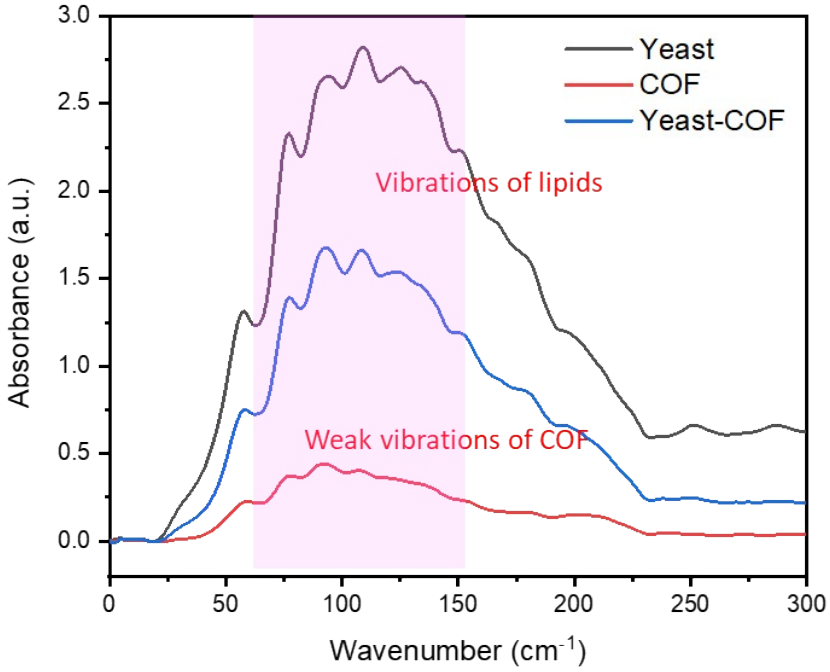

Figure S7. Synchrotron THz/Far-IR spectra of native yeast, COF, and yeast-COF.

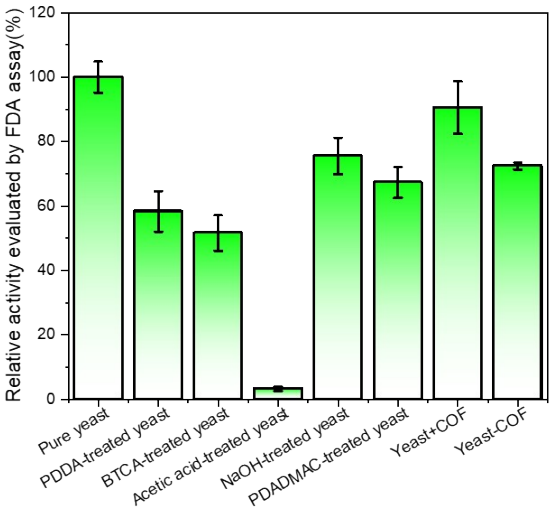

Figure S8. Cell activity evaluated by FDA assay upon different precursors treatment.

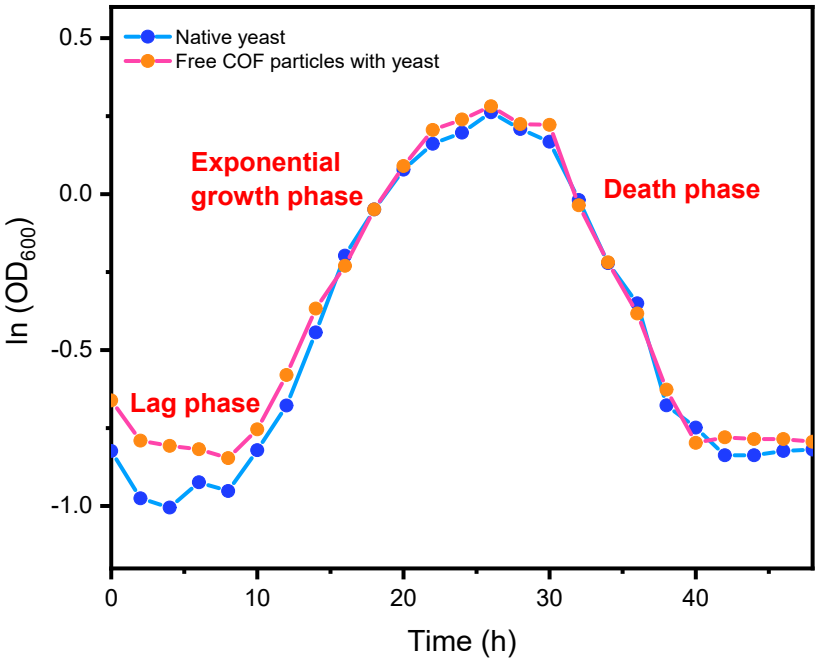

Figure S9. Yeast growth measurement (OD_{600}) for native yeasts and yeasts in the presence of free COF-LZU1 particles.

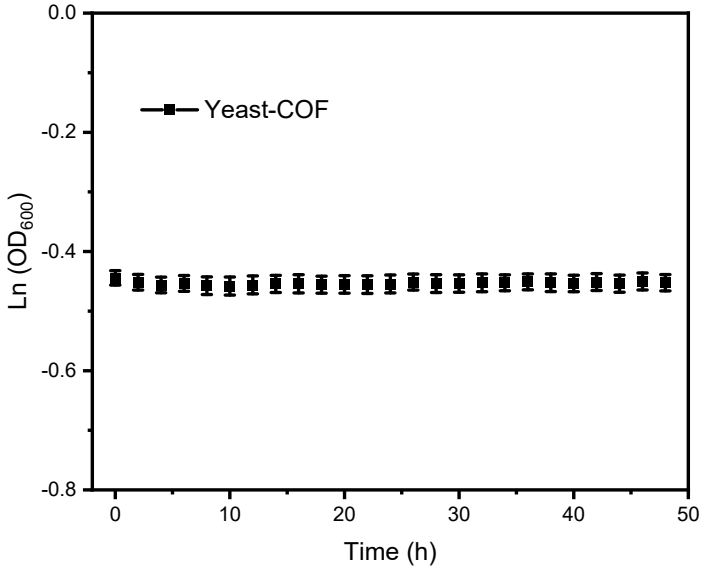

Figure S10. Yeast growth measurement (OD_{600}) for yeast-COF.

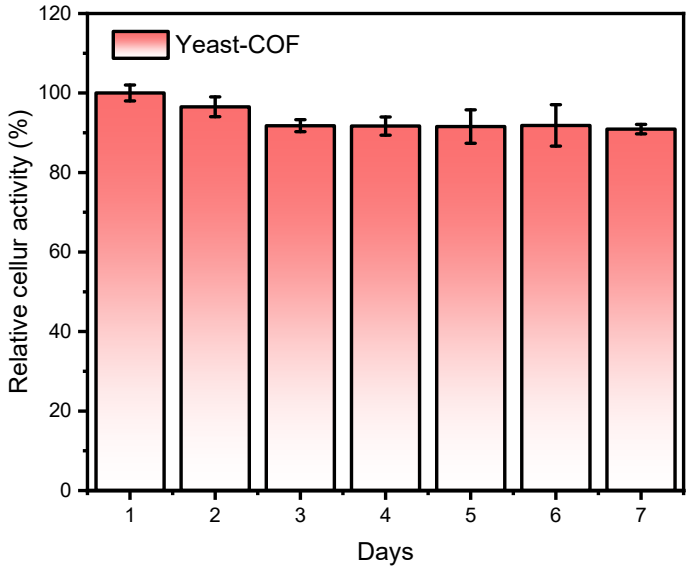

Figure S11. The relative cellular activity of yeast-COF after incubation in a cell medium for a week.

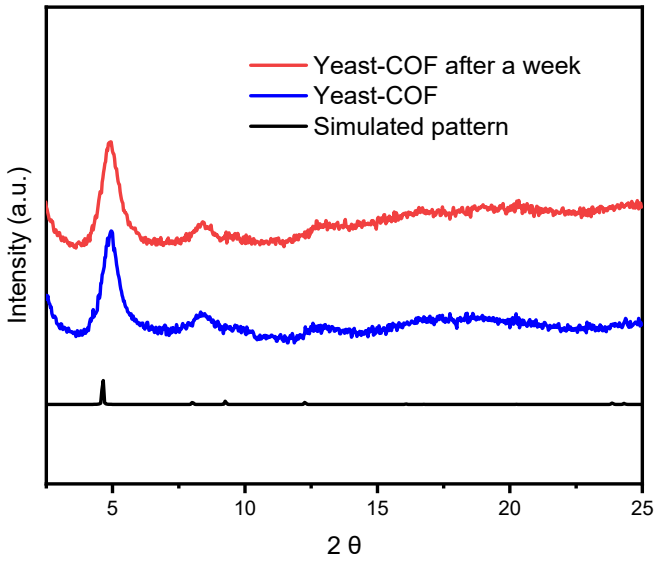

Figure S12. XRD spectra after incubation in the cell medium for a week.

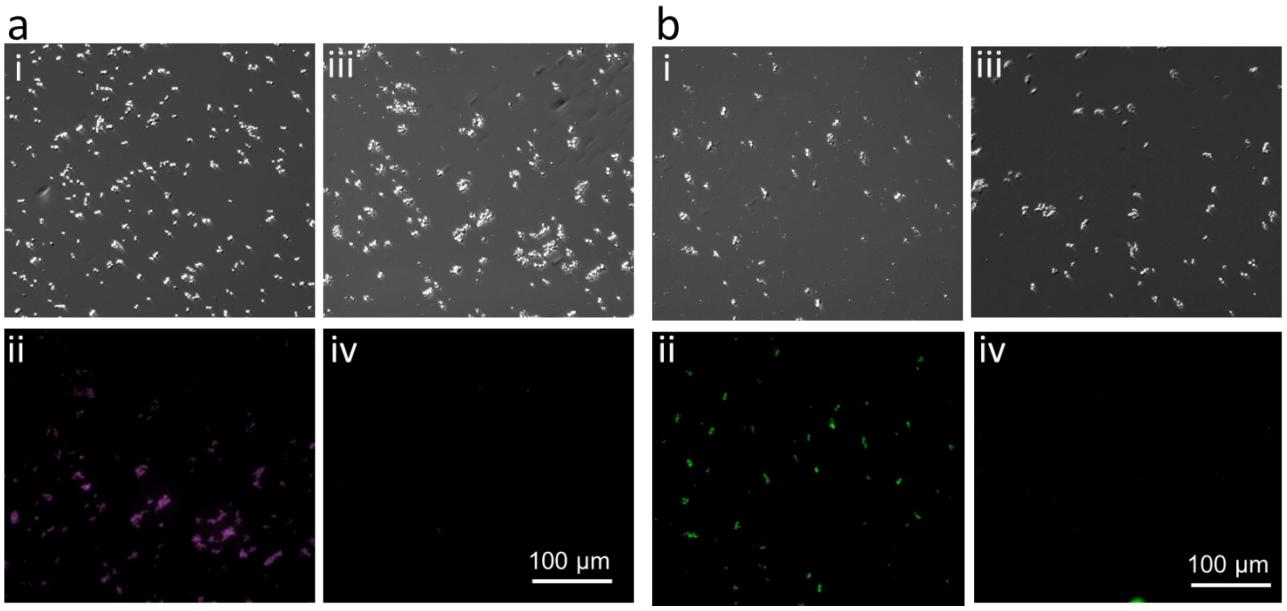

Figure S13. Cell activity evaluated by (a) resazurin assay and (b) FDA assay on (i, ii) yeast-COF and (iii, iv) native yeast cells upon high temperature treatment at 75 °C for 30 min.

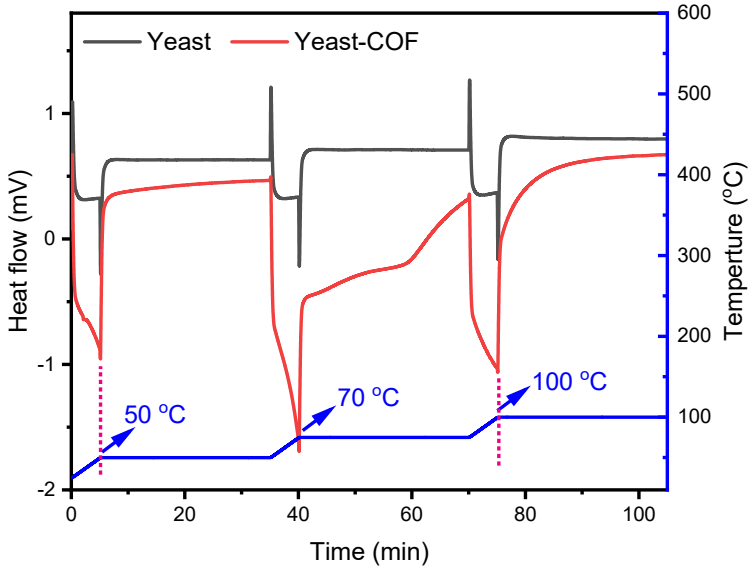

Figure S14. DSC analysis of native yeast and yeast-COF cells at 50 °C, 75 °C and 100 °C. Yeast-COF exhibited the greater heat flow, indicating that the COF shells effectively reradiate incident heat energy. The blue curve is the increased temperature with time.

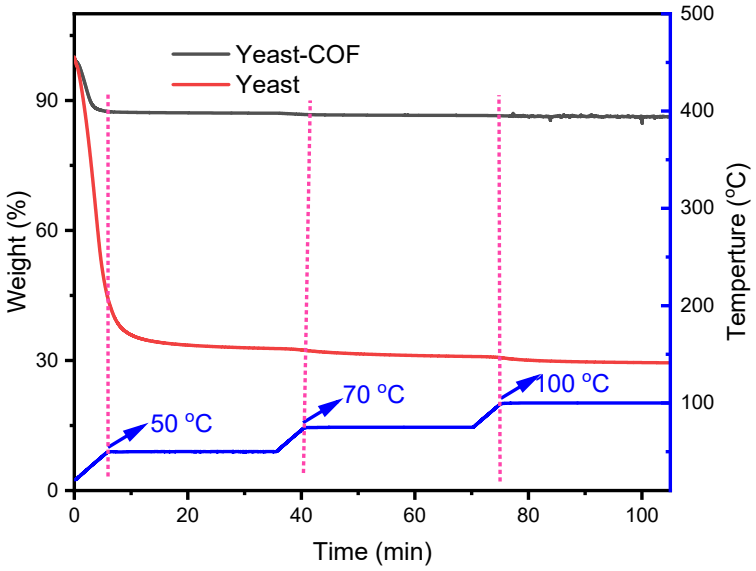

Figure S15. TGA analysis of native yeast and yeast-COF cells at 50 °C, 75 °C and 100 °C. The blue curve is the increased temperature with time.

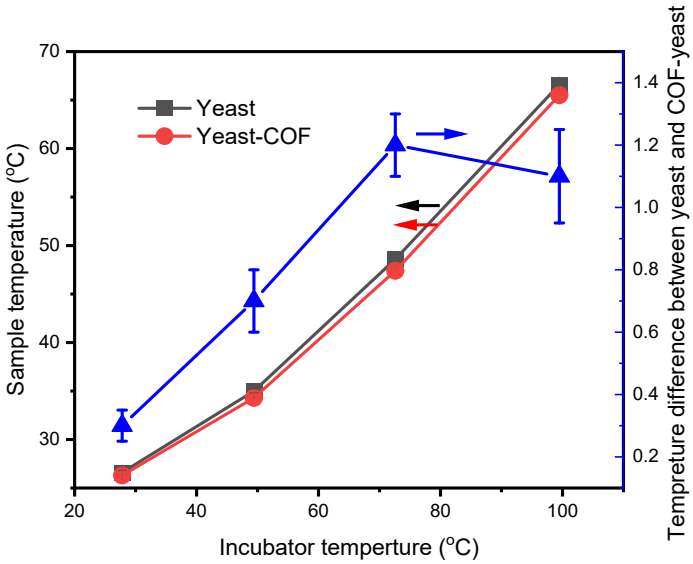

Figure S16. Sample surface temperatures and temperature difference obtained from native yeast and yeast-COF exposed to a range of temperatures (~30 to 100 °C).

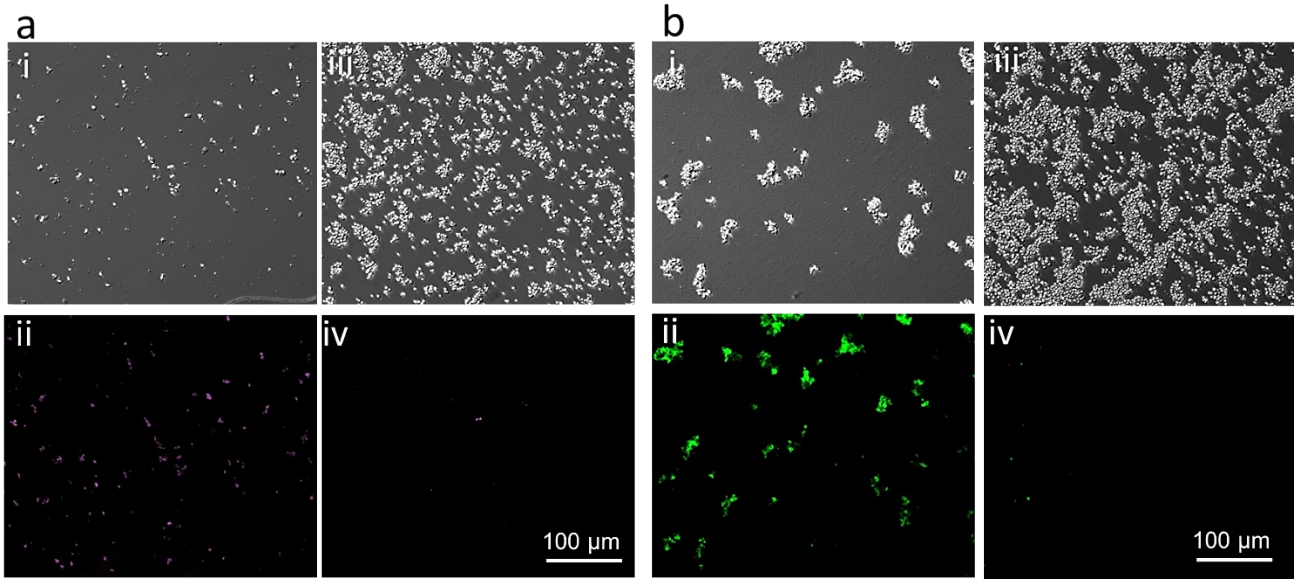

Figure S17. Cell activity evaluated by (a) resazurin assay and (b) FDA assay on (i, ii) yeast-COFand (iii, iv) native yeast cells upon pH 2 treatment for one hour.

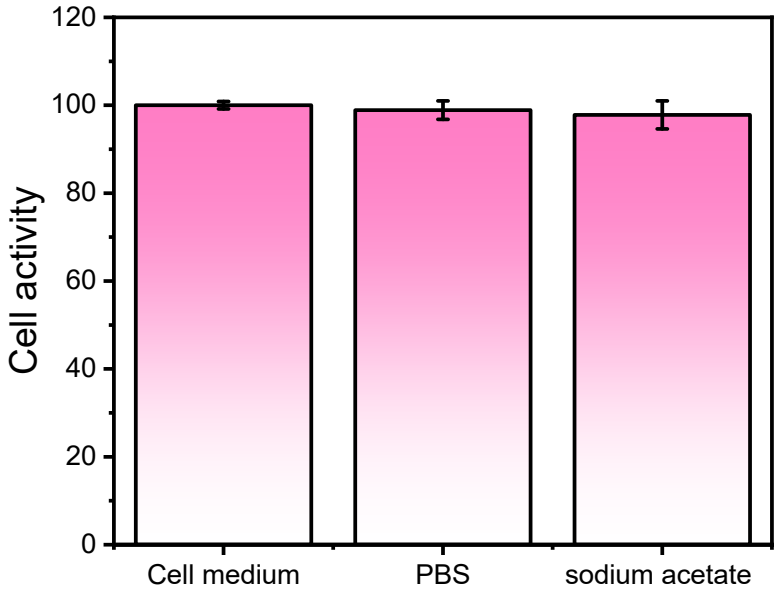

Figure S18. Cell activity evaluated by resazurin assay upon different buffer salt.

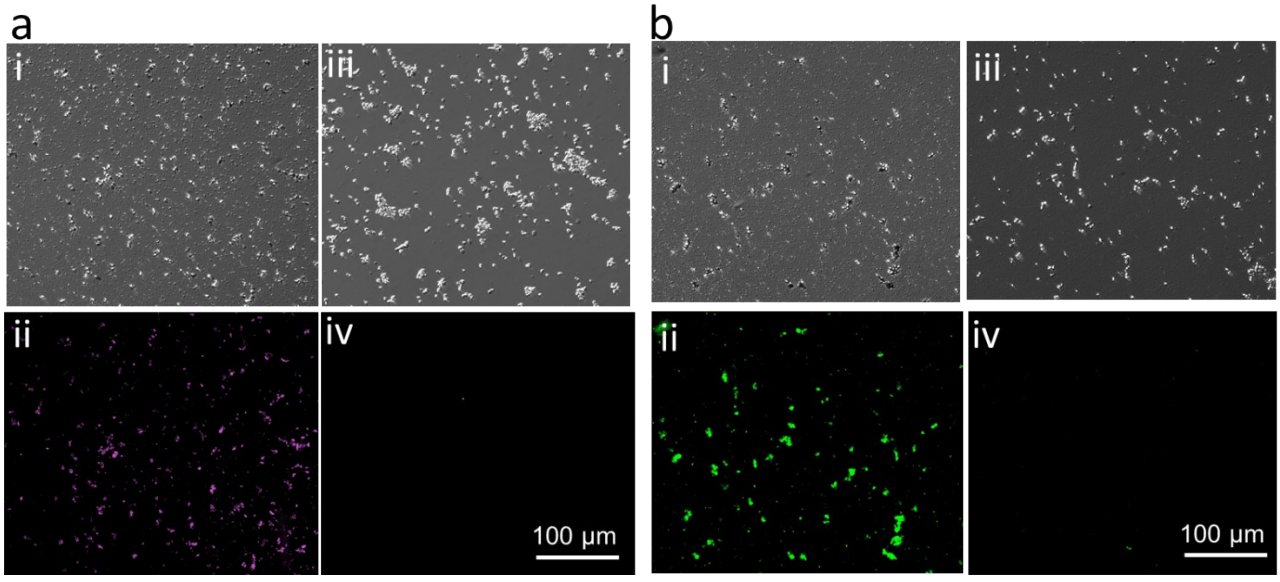

Figure S19. Cell activity evaluated by (a) resazurin assay and (b) FDA assay on (i, ii) yeast-COF and (iii, iv) native yeast cells upon UV irradiation (254 nm) for four hours.

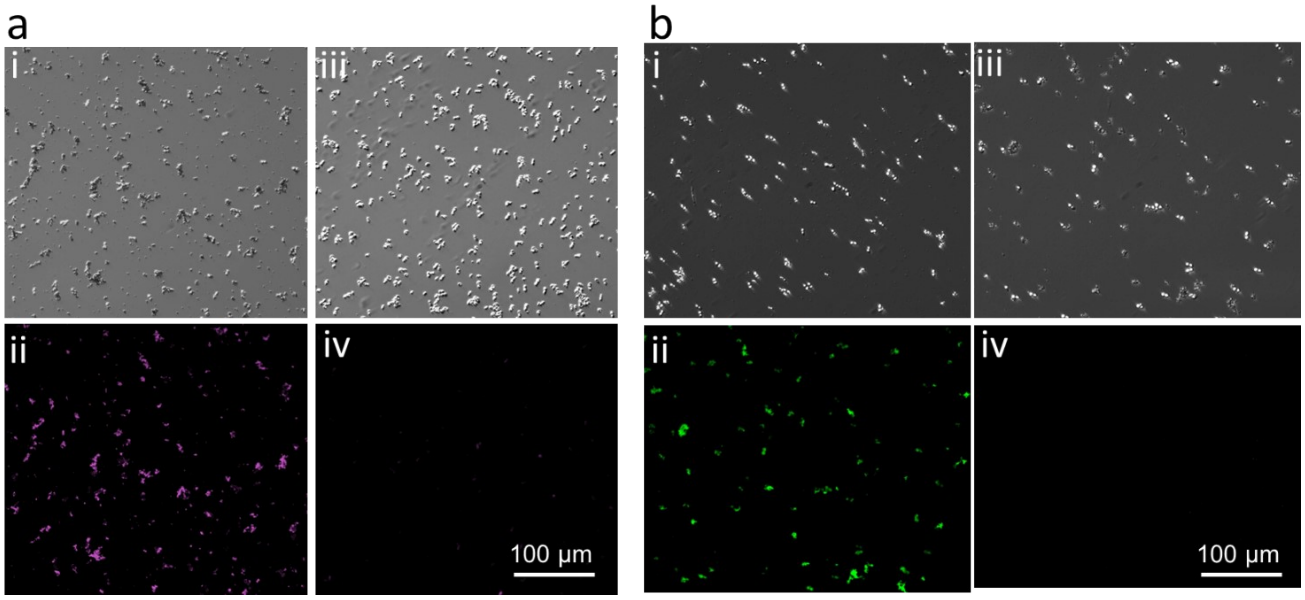

Figure S20. Cell activity evaluated by (a) resazurin assay and (b) FDA assay on (i, ii) yeast-COF and (iii, iv) native yeast cells upon 1M $CuCl_2$ treatment for one hour.

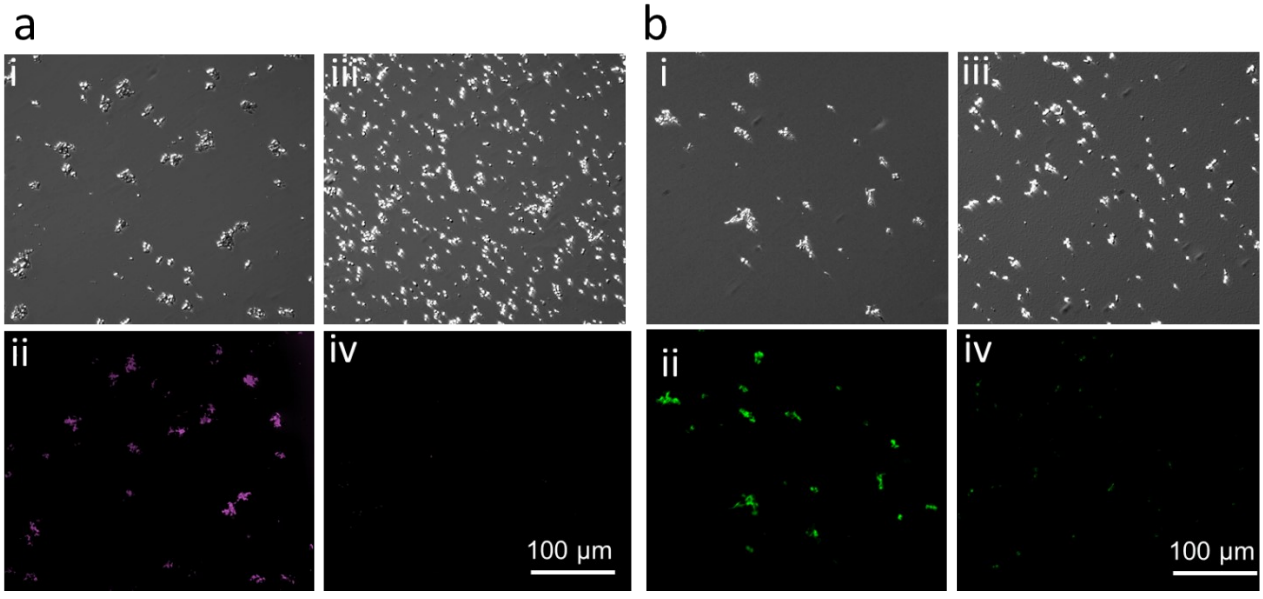

Figure S21. Cell activity evaluated by (a) resazurin assay and (b) FDA assay on (i, ii) yeast-COF and (iii, iv) native yeast cells upon 500 mM H_2O_2 treatment for one hour.

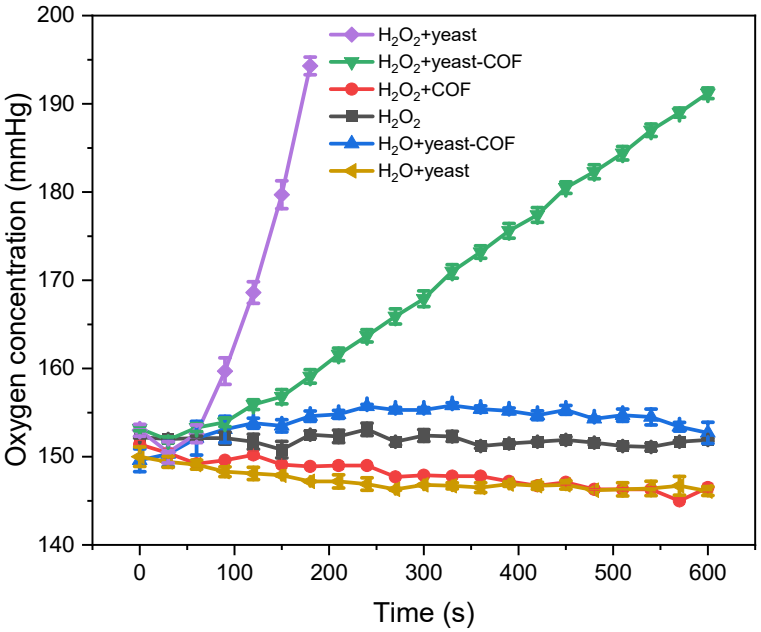

Figure S22. Oxygen concentration under different conditions in the condition of 100 mM H_2O_2.

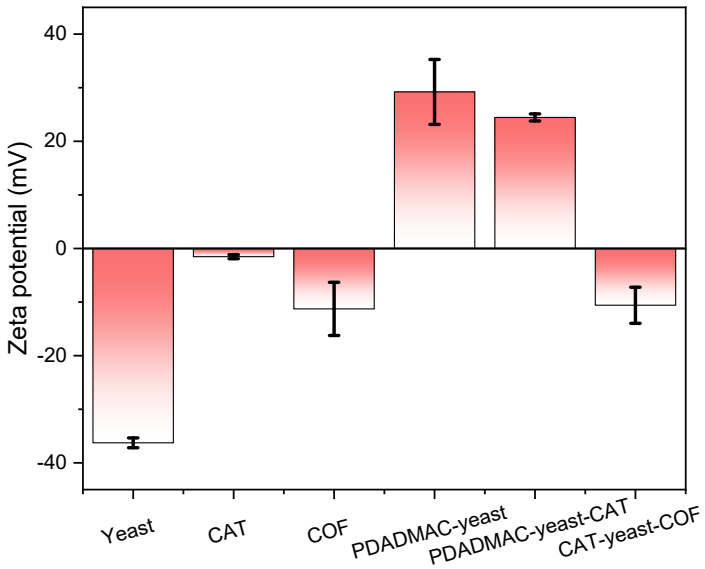

Figure S23. The zeta potential of the samples during the CAT-yeast-COF synthetic process.

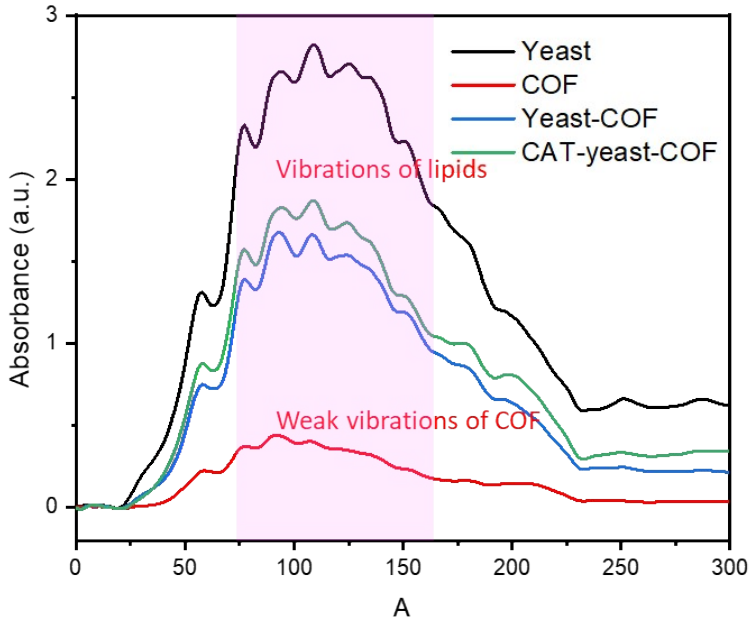

Figure S24. Synchrotron THz/Far-IR spectra of CAT-yeast-COF in comparison with other samples.

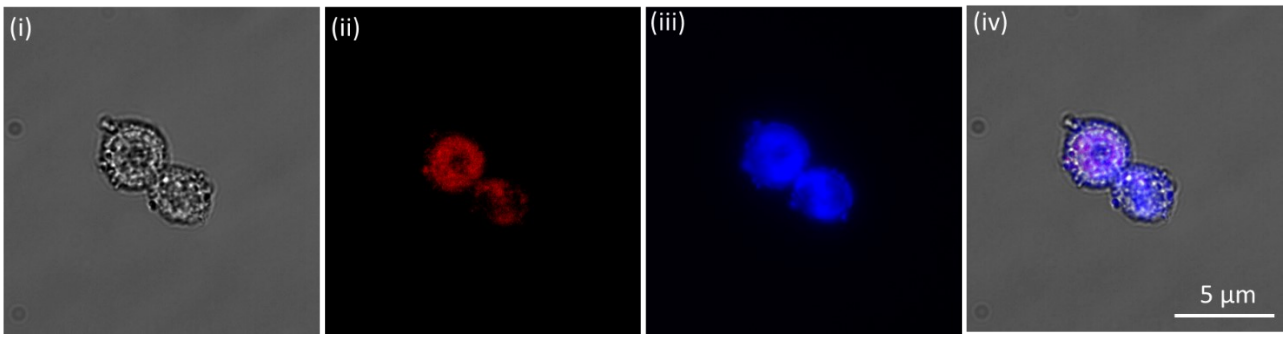

Figure S25. The homogeneous formation of the CAT-COF-based exoskeleton around yeast. (i) bright filed image; (ii) Fluorescent image of Atto 647N NHS ester-labelled CAT (red); (iii) Fluorescent image of Alexa Fluor 350-labelled COF-LZU1 (blue); (iv) The mixture image of (i), (ii) and (iii). The enzyme loading efficiency is 50.0%, which is calculated by subtracting the Alexa Fluor 350 in the supernatant after synthesis.

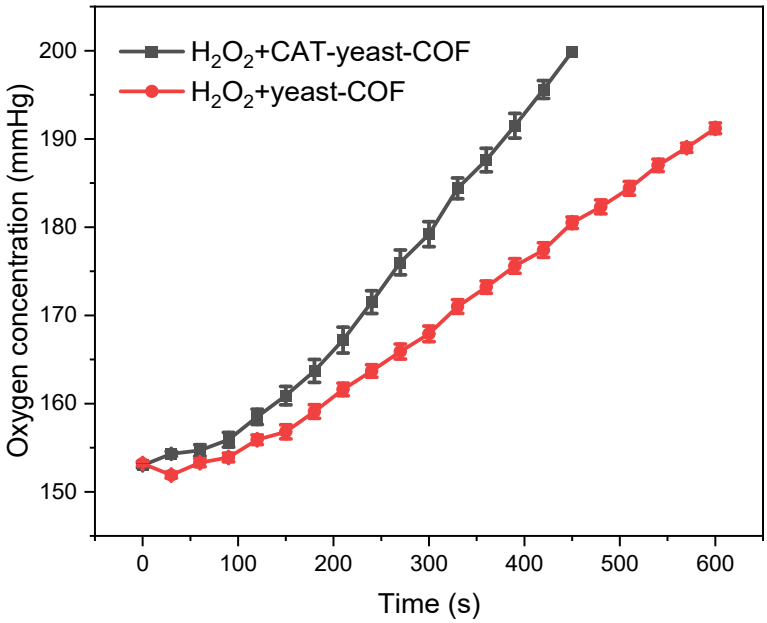

Figure S26. Oxygen concentration produced by CAT-yeast-COF and yeast-COF in the condition of 100 mM H_2O_2.

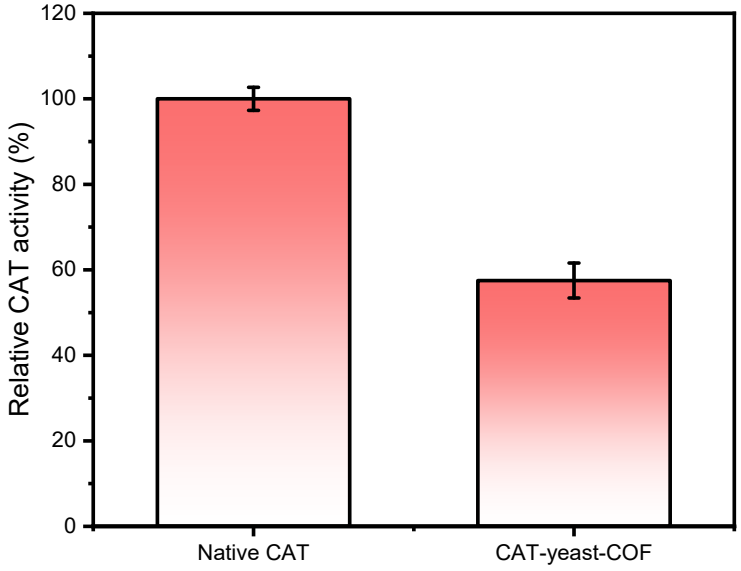

Figure S27. Relative CAT activity upon immobilization on the yeast-COF.

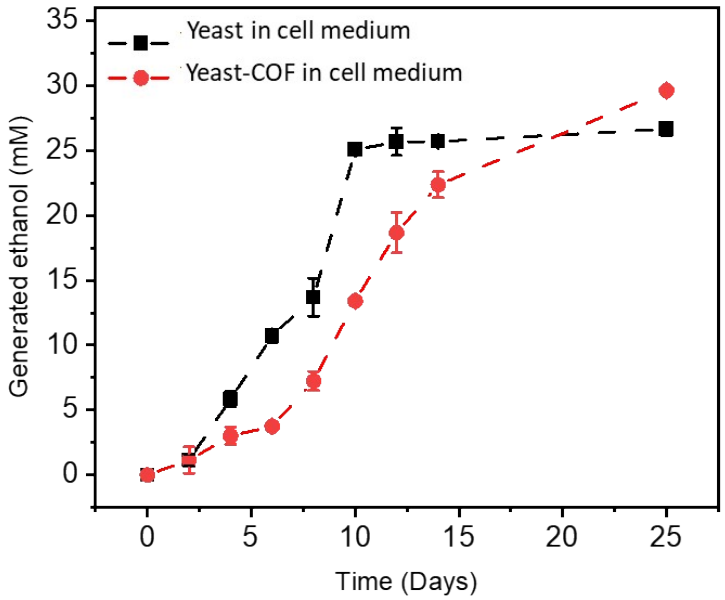

Figure S28. Ethanol production of bare yeast and yeast-COF under the cell media for 25 days.

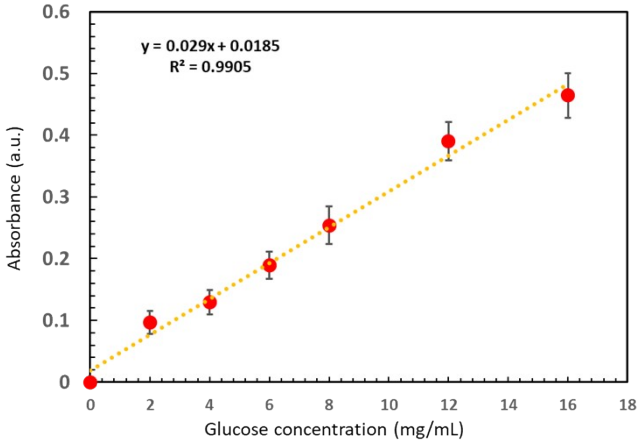

Figure S29. Glucose standard curves in the range of 0-16 mg/mL.

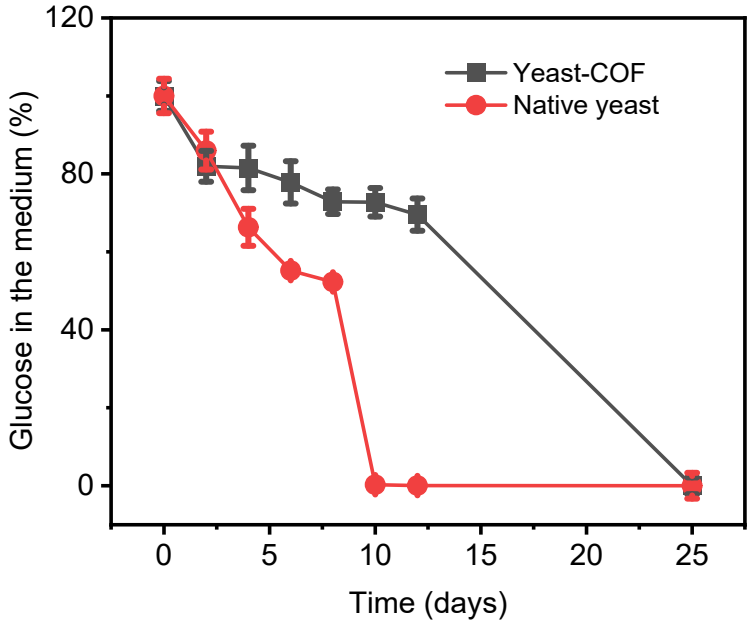

Figure S30. Retention of glucose in the culture medium during fermentation for 25 days.

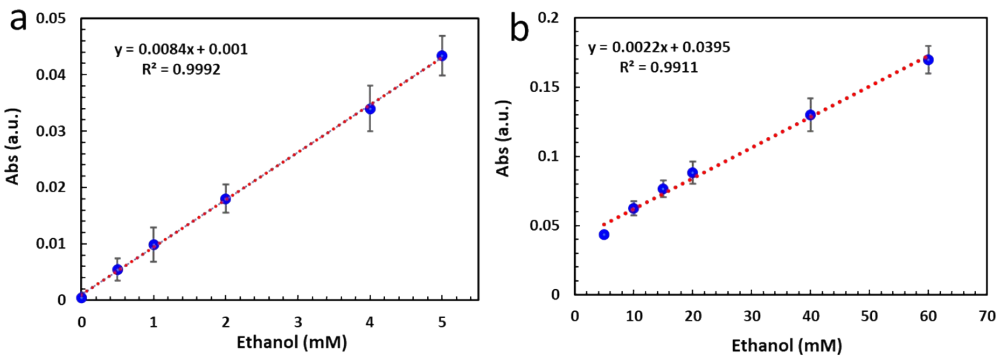

Figure S31. Ethanol standard curves in the range of (a) 0-5 mM and (b) 5-60 mM.

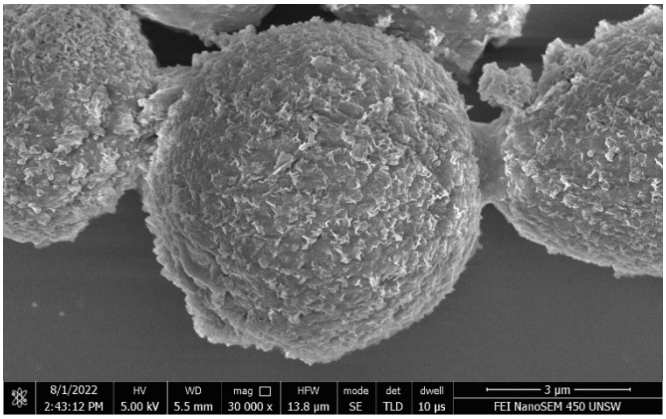

Figure S32. SEM image of yeast-ZIF-8.

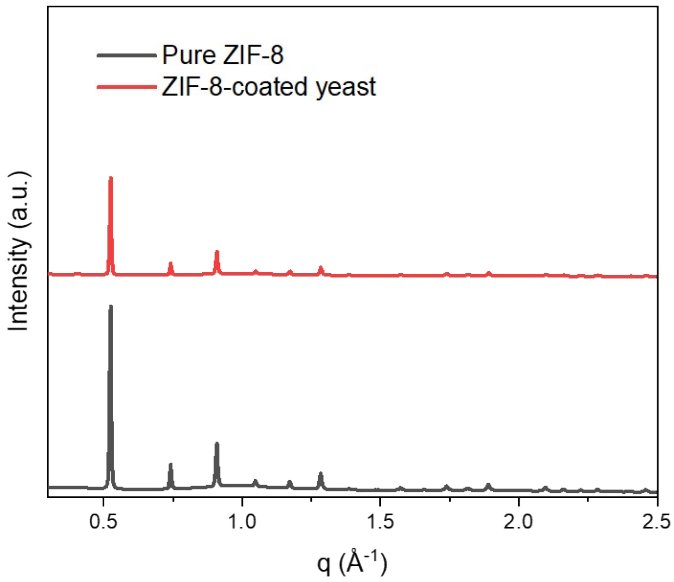

Figure S33. SAXS spectra of pure ZIF-8 and yeast-ZIF-8.

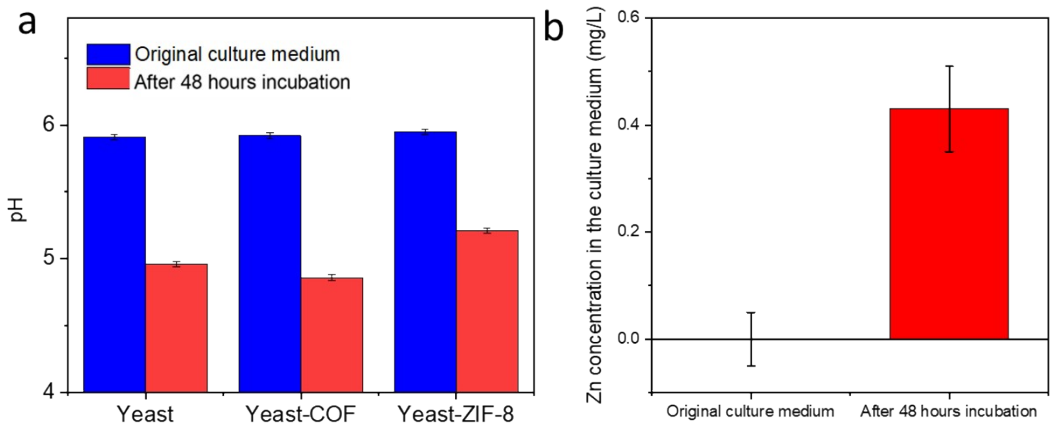

Figure S34. (a) pH of yeast, yeast-COF and yeast-ZIF-8 in cell medium before and after incubation for 48 hours. (b) ICP result of cell medium after incubation with the yeast-ZIF-8 for 48 hours.

References:

[1] J. Liang, J. Ruan, B. Njegic, A. Rawal, J. Scott, J. Xu, C. Boyer and K. Liang, Insight into Bioactivity of In-situ Trapped Enzyme-Covalent-organic Frameworks, *Angew. Chem. Int. Ed.*, 2023, e202303001.
[2] K. Liang, J. J. Richardson, J. Cui, F. Caruso, C. J. Doonan and P. Falcaro, Metal–Organic Framework Coatings as Cytoprotective Exoskeletons for Living Cells, *Adv. Mater.*, 2016, **28**, 7910-7914.
[3] K. Liang, J. J. Richardson, C. J. Doonan, X. Mulet, Y. Ju, J. Cui, F. Caruso and P. Falcaro, An Enzyme-Coated Metal–Organic Framework Shell for Synthetically Adaptive Cell Survival, *Angew. Chem. Int. Ed.*, 2017, **56**, 8510-8515.
[4] Z. Ji, H. Zhang, H. Liu, O. M. Yaghi and P. Yang, Cytoprotective metal-organic frameworks for anaerobic bacteria, *PNAS*, 2018, **115**, 10582-10587.
[5] L. Shi, A. Li, W. Zhang, H. Wu and Y. Chi, Endowing chloroplasts with artificial "cell walls" using metal–organic frameworks, *Nanoscale*, 2020, **12**, 11582-11592.
[6] J. H. Park, K. Kim, J. Lee, J. Y. Choi, D. Hong, S. H. Yang, F. Caruso, Y. Lee and I. S. Choi, A Cytoprotective and Degradable Metal–Polyphenol Nanoshell for Single-Cell Encapsulation, *Angew. Chem. Int. Ed.*, 2014, **53**, 12420-12425.
[7] B.J. Kim, T. Park, H.C. Moon, S.Y. Park, D. Hong, E.H. Ko, J.Y. Kim, J.W. Hong, S.W. Han, Y.G. Kim, I.S. Choi. Cytoprotective Alginate/Polydopamine Core/Shell Microcapsules in Microbial Encapsulation, *Angew. Chem. Int. Ed*, 2014, **53**, 14443-14446.
[8] G. Wang, L. Wang, P. Liu, Y. Yan, X. Xu and R. Tang Extracellular Silica Nanocoat Confers Thermotolerance on Individual Cells: A Case Study of Material-Based Functionalization of Living Cells, *ChemBioChem*, 2010, **11**, 2368-2373.

[9] E. H. Ko, Y. Yoon, J. H. Park, S. H. Yang, D. Hong, K.-B. Lee, H. K. Shon, T. G. Lee and I. S. Choi, Bioinspired, Cytocompatible Mineralization of Silica–Titania Composites: Thermoprotective Nanoshell Formation for Individual Chlorella Cells, *Angew. Chem. Int. Ed.*, 2013, **52**, 12279-12282.
[10] A. I. Zamaleeva, I. R. Sharipova, A. V. Porfireva, G. A. Evtugyn, R. F. Fakhrullin. Polyelectrolyte-Mediated Assembly of Multiwalled Carbon Nanotubes on Living Yeast Cells. *Langmuir.,* 2010, **26**, 4, 2671–2679.